Int. J. Radiation Oncology Biol. Phys., Vol. 76, No. 3, pp. 949–955, 2010

0360-3016/10/$–see front matter

doi:10.1016/j.ijrobp.2009.07.004

PHYSICS CONTRIBUTION

CONE-BEAM CT ASSESSMENT OF INTERFRACTION AND INTRAFRACTION SETUP ERROR OF TWO HEAD-AND-NECK CANCER THERMOPLASTIC MASKS

Michael Velec, B.Sc.,* John N. Waldron, M.D.,*† Brian O'Sullivan, M.D.,*† Andrew Bayley, M.D.,*† Bernard Cummings, M.B.,*† John J. Kim, M.D.,*† Jolie Ringash, M.D.,*† Stephen L. Breen, Ph.D.,*† Gina A. Lockwood, M.Math.,‡ and Laura A. Dawson, M.D.*†

*Radiation Medicine Program and ‡Department of Biostatistics, Princess Margaret Hospital, University Health Network, Toronto, Ontario, Canada; and †Department of Radiation Oncology, University of Toronto, Toronto, Ontario, Canada

Purpose: To prospectively compare setup error in standard thermoplastic masks and skin-sparing masks (SSMs) modified with low neck cutouts for head-and-neck intensity-modulated radiation therapy (IMRT) patients.
Methods and Materials: Twenty head-and-neck IMRT patients were randomized to be treated in a standard mask (SM) or SSM. Cone-beam computed tomography (CBCT) scans, acquired daily after both initial setup and any repositioning, were used for initial and residual interfraction evaluation, respectively. Weekly, post-IMRT CBCT scans were acquired for intrafraction setup evaluation. The population random (σ) and systematic (Σ) errors were compared for SMs and SSMs. Skin toxicity was recorded weekly by use of Radiation Therapy Oncology Group criteria.
Results: We evaluated 762 CBCT scans in 11 patients randomized to the SM and 9 to the SSM. Initial interfraction σ was 1.6 mm or less or 1.1° or less for SM and 2.0 mm or less and 0.8° for SSM. Initial interfraction Σ was 1.0 mm or less or 1.4° or less for SM and 1.1 mm or less or 0.9° or less for SSM. These errors were reduced before IMRT with CBCT image guidance with no significant differences in residual interfraction or intrafraction uncertainties between SMs and SSMs. Intrafraction σ and Σ were less than 1 mm and less than 1° for both masks. Less severe skin reactions were observed in the cutout regions of the SSM compared with non-cutout regions.
Conclusions: Interfraction and intrafraction setup error is not significantly different for SSMs and conventional masks in head-and-neck radiation therapy. Mask cutouts should be considered for these patients in an effort to reduce skin toxicity. © 2010 Elsevier Inc.

Cone-beam CT, Image guidance, Head-and-neck cancer, Immobilization.

INTRODUCTION

Highly conformal radiotherapy techniques such as intensity-modulated radiation therapy (IMRT) have been shown to reduce xerostomia and improve quality of life in head-and-neck cancer patients (1, 2). Because IMRT plans are more sensitive to uncertainties due to positioning (3, 4), geometric errors should be considered in treatment planning or planning target volume design. Immobilization of the head and neck is mandated to maintain the patient's position during and between treatment fractions.

Benefits of thermoplastic immobilization include their noninvasive nature, ease of fabrication, and quick setup time. Thermoplastic masks have previously been shown in both prospective randomized and retrospective studies to have setup accuracy on the order of a few millimeters (5–12). The majority of the original studies investigating setup error relied on the alignment of two-dimensional images such as megavoltage portal films to a reference digitally reconstructed radiograph, as opposed to a three-dimensional (3D) volumetric registration such as cone-beam computed tomography (CBCT) to a planning computed tomography (CT) scan. Calculated setup errors between two-dimensional images may not be equivalent to errors found by registering 3D to 3D volumes (13). In addition to setup error, repeat CT imaging studies have shown substantial changes in head-and-neck anatomy due to neck flexion and changes in tumor volume, shape, and position (14–16).

Reprint requests to: Laura A. Dawson, M.D., Department of Radiation Oncology, Princess Margaret Hospital, 610 University Ave., Toronto, ON M5G 2M9 Canada. Tel: (416) 946-2125; Fax: (416) 946-6566; E-mail: laura.dawson@rmp.uhn.on.ca

Presented in part at the 49th Annual Meeting of the American Society for Therapeutic Radiology and Oncology, October 28–November 1, 2007, Los Angeles, CA.

Conflict of interest: none.

Acknowledgments—The authors thank the radiation therapists of the head-and-neck site group for carrying out the study procedures, Graham Wilson for information technology support, Bruna Ariganello for contribution to the figures, and Bern Norrlinger and David Hwang for help with this study.

Received Jan 23, 2009, and in revised form July 1, 2009. Accepted for publication July 1, 2009.

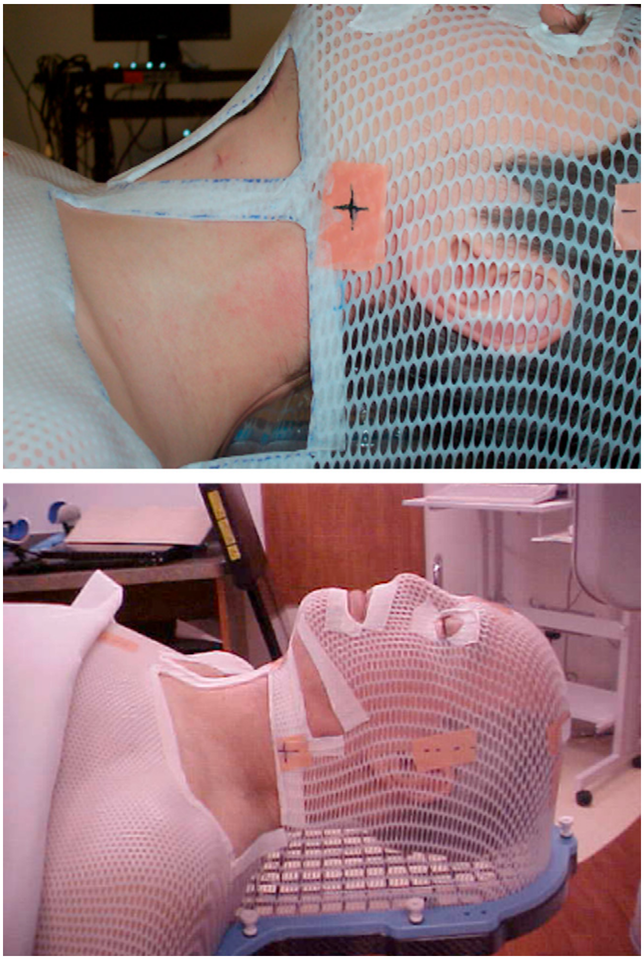

Fig. 1. Two examples of patients receiving treatment with low-neck mask cutouts.

A disadvantage of thermoplastic immobilization is a reduction of the skin-sparing effect awarded by megavoltage irradiation (17). Surface dose increases of 14% to 40% on phantoms under 2 mm of thermoplastic material with 6-MV photons have been reported (18–21). Lee *et al.* (22) showed that head-and-neck IMRT is not immune to this effect because both conventional and IMRT plans had a mean surface dose increase of 18% for 3-mm thermoplastic masks, an increase sufficient to cause substantial skin reactions. Stretching the mask during fabrication can reduce the amount of skin dose received (17, 23), particularly in the neck region, which is prone to having the thickest layer after fabrication. The development of treatment approaches that reduce the dose to the skin is therefore warranted in regions away from the gross tumor volumes.

Cutting out portions of thermoplastic material has been proposed as a method to potentially reduce skin reactions due to the removal of the bolus effect. We hypothesized that cutting the mask in the neck area below the angle of the jaw may be done without substantial change in intrafraction and interfraction setup variability. Before implementing skin-sparing masks (SSMs) for our head-and-neck IMRT patients, a study was designed to measure the changes in setup error that may occur by introducing cutouts into standard thermoplastic masks. Similar masks have been investigated by Weltens *et al.* (24), where treatment portal cutouts did not affect reproducibility compared with intact masks, when examining orthogonal portal films. No volumetric studies of daily setup error in patients with mask cutouts have been published.

The aim of this study is to prospectively compare the interfraction errors of standard head-and-shoulder thermoplastic masks with masks with low neck cutouts aimed at reducing acute skin reactions. Setup errors were measured on daily CBCT scans acquired at each fraction under an image-guided radiotherapy (IGRT) treatment protocol. The secondary aims were to assess intrafraction setup change and clinical acute skin toxicity.

METHODS AND MATERIALS

This institutional ethics review board–approved study was conducted from April 2006 to January 2008. Eligible patients for this study included those with head-and-neck cancer who we planned to treat with IMRT (≥20 fractions) and daily CBCT image guidance. Patients were excluded if the use of bolus material was planned or if mask cutouts were required for non-study purposes, such as for tracheostomies or mouth bites. Potential patients were approached, consented, and were randomized on the day of their CT simulation and mask-fabrication appointments. We planned to enroll 20 patients in the study and randomize them to be treated in the standard mask (SM) or an SSM.

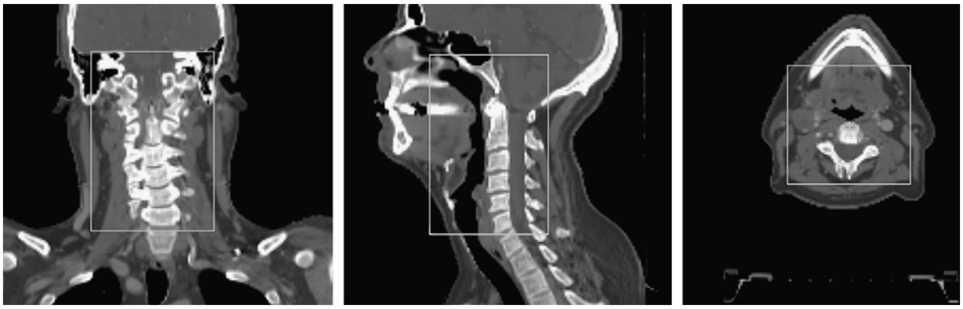

Fig. 2. Example of a clip box (white) overlaid on the planning computed tomography scan in the coronal (left), sagittal (middle), and axial (right) planes.

Table 1. Patient demographics

	SM (n = 11)	SSM (n = 9)
Age [median (range)] (y)	58 (43–77)	56 (23–66)
Gender (M/F)	10/1	9/0
Primary tumor site (%)		
Oropharynx	3 (27.3)	7 (77.8)
Larynx	2 (18.2)	1 (11.1)
Oral cavity	2 (18.2)	0
Salivary gland	0	1 (11.1)
Nasopharynx	2 (18.2)	0
Unknown	2 (18.2)	0
Dose and fractionation (%)		
70 Gy in 35 fractions	4 (36.4)	5 (55.6)
66 Gy in 33 fractions	0	1 (11.1)
64 Gy in 40 fractions twice daily	2 (18.2)	2 (22.2)
60 Gy in 30 fractions	1 (9.1)	1 (11.1)
60 Gy in 25 fractions	4 (36.4)	0
Concurrent chemotherapy (%)	3 (27.2)	4 (44.4)

Abbreviations: SM = standard mask; SSM = skin-sparing mask.

Immobilization devices

All patients were immobilized in thermoplastic head-and-shoulder masks (WFR/Aquaplast, Wyckoff, NJ). Masks made of 2.4-mm-thick perforated thermoplastic material were locked into the CT simulator or linear accelerator tables through nine fixation points. Reusable neck rests from a standard set were chosen to best conform to the patient's neck. Isocenter location was determined at CT simulation after fabrication and marked on the mask. A tattoo was placed on the superior sternum in line with the isocenter to aid with patient straightening.

Masks in both groups were cut out around the eyes and lips on the first day before treatment. The group with the SM received no additional mask cutouts. The SSM group received additional cutouts in the bilateral lower neck. This region typically extended from the mandible inferiorly down to the clavicle and laterally encompassing the supraclavicular fossa (Fig. 1). Strips of mask were left intact midline and along planes of the isocenter to aid in room setup with lasers. Care was taken not to cut regions that are thought to contribute to setup reproducibility such as over the humeral head, chin, bridge of the nose, and so on. Attempts were made to ensure that patterns of SSM cutouts were equal between patients, although variations exist because of initial isocenter placement.

Setup and image guidance

Daily initial setup consisted of aligning in-room lasers with mask marks and chest tattoos. A volumetric kilovoltage CBCT scan was then acquired with a linear accelerator–mounted X-ray source (Synergy; Elekta AB, Stockholm, Sweden) (25). Images were assessed online by the radiation therapists by fusing the CBCT scan to the planning CT scan using the commercially available software. An automated bony registration algorithm was used considering anatomy in the ''clip box'' or user-defined registration volume. This typically extended from the clivus to C6 vertebrae and included high-dose regions of interest and organs at risk (Fig. 2). Registration was thus based primarily on vertebral body alignment, although results were visually inspected by the therapists and manual adjustments were made if necessary to provide the best fit.

Setup corrections were made via couch shifts if the initial translational error was greater than 4 mm for the first 2 patients and greater than 3 mm for all subsequent patients, because of a change in our routine IGRT policy. Patients were also repositioned in the mask and reimaged if rotations greater than 3° existed in any plane or if large deformations were observed. A verification CBCT scan was repeated and assessed for residual error after any corrections or repositioning done before IMRT delivery. Radiation therapists made offline systematic setup corrections by re-marking the isocenter on the mask if trends in the initial setup error of 2 mm or greater were observed over at least 3 consecutive fractions. For research purposes, weekly CBCT scans were also acquired immediately after IMRT delivery for offline analysis of intrafraction movement.

CBCT image analysis

All CBCT images were assessed offline by a single observer (M.V.) replicating the online image-matching strategy. The 3D setup error about the isocenter was evaluated in 6 degrees of freedom (*df*) with translational error as medial–lateral (ML), cranial–caudal (CC), and anterior–posterior (AP) and rotational error as pitch, roll, and yaw. The first daily CBCT scan after in-room setup, before corrections or treatment, was used to calculate the initial interfraction error. The final daily CBCT scan acquired before treatment after any corrections was used to calculate the residual interfraction error. Cone-beam CT images for fractions where the initial setup was within tolerance and no corrective action was done were used in both the initial and residual interfraction calculations. Intrafraction setup error was measured by comparing the final and postfraction CBCT scans. Intraobserver variability was estimated by repeating measurements on 5% of the acquired images.

Population random error (σ) and the distribution of systematic errors (Σ) were calculated for both SM and SSM groups, by use of definitions from van Herk (26). This was done for interfraction and intrafraction error. Population random error (σ) was calculated by use of the root–mean–square of the individual patient SDs, and

Table 2. Interfraction and intrafraction error for both mask groups in terms of random (σ) and systematic (Σ) components

	Initial interfraction error				Residual interfraction error				Residual intrafraction error			
	SM		SSM		SM		SSM		SM		SSM	
	σ	Σ	σ	Σ	σ	Σ	σ	Σ	σ	Σ	σ	Σ
ML (mm)	1.5	0.8	1.3	0.8	1.3	0.7	1.2	0.6	0.8	0.3	0.8	0.7
CC (mm)	1.5	1.0	2.0	1.1	1.3	0.8	1.5	0.6	0.7	0.5	0.8	0.5
AP (mm)	1.6	1.0	1.6	0.8	1.3	0.8	1.3	0.7	0.8	0.7	0.9	0.7
Pitch (°)	0.9	0.9	0.8	0.8	0.8	0.9	0.8	0.8	0.7	0.3	0.6	0.3
Roll (°)	1.1	1.4	0.8	0.6	0.8	1.5	0.8	0.6	0.7	0.5	0.8	0.5
Yaw (°)	0.9	0.9	0.8	0.9	0.8	0.9	0.8	0.9	0.6	0.4	0.8	0.4

Abbreviations: SM = standard mask; SSM = skin-sparing mask; ML = medial–lateral; CC = cranial–caudal; AP = anterior–posterior.

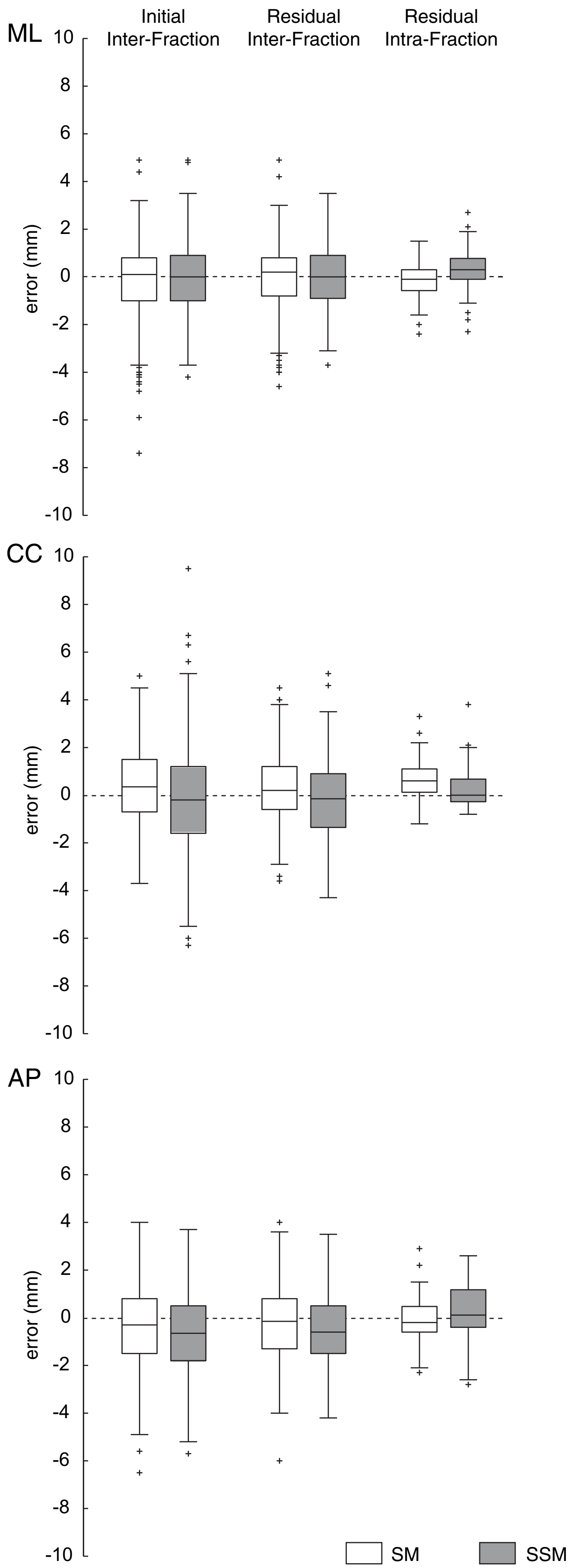

the distribution of systematic errors (Σ) by use of the SD of the individual mean errors.

Skin toxicity assessment

Acute skin reactions in the treatment area were examined and documented weekly in the patients' charts by radiation oncologists and radiation therapists who specialized in head-and-neck cancer radiotherapy. Skin toxicity was graded weekly during radiation therapy, by use of the Radiation Therapy Oncology Group Acute Morbidity Scoring Criteria. The oncologists' grading was preferred over the therapists', and if any weekly toxicity grading was missing, skin assessments documented with descriptive notes (*i.e.*, bright erythema) were converted into a Radiation Therapy Oncology Group score (by M.V.). A follow-up score up to 3 months after the completion of radiotherapy was also recorded if available. A Cochran-Armitage test for trend (exact) was used to compare toxicity trends between groups.

RESULTS

Between April 2006 and January 2008, 20 patients were enrolled and randomized in the study. Eleven patients received treatment with the SM and nine with the SSM. Patient demographics and treatment prescriptions are shown in Table 1. All patients were treated with IMRT plans ranging from 5 to 10 (median, 9) coplanar 6-MV beams. Cone-beam CT images from 20 patients were evaluated, including 644 pre-IMRT images (338 SM and 306 SSM) and 118 post-IMRT images (59 SM and 59 SSM).

There were no significant differences in interfraction or intrafraction setup errors between the SM and SSM, as shown in Table 2 and Fig. 3. Reproducibility of the setup for each mask is shown in Table 3. When evaluating the initial CBCT, we found that errors greater than 3 mm in any plane were seen 22.2% of the time for the SM vs. 24.8% of the time for the SSM. Errors greater than 5 mm were seen 1.2% of the time for the SM and 3.6% of the time for the SSM. After setup corrections via couch shifts, or repositioning, these rates were reduced to approximately 10% for errors greater than 3 mm and less than 1% for errors greater than 5 mm for both SM and SSM groups. Patients in the SM group had to be completely repositioned in their masks 3% of the time after CBCT imaging vs. 1% in the SSM group.

To assess intraobserver variability, we re-evaluated 43 random CBCT scans after subject accrual was complete. SDs (mean) of the difference between the repeat registrations were 0.5 mm (0.0 mm), 0.5 mm (0.1 mm), and 0.7 mm (0.1 mm) in the ML, CC, and AP directions, respectively, and 0.6° (0.0°), 0.6° (0.0°), and 0.6° (−0.1°) for pitch, roll, and yaw, respectively.

The highest-graded acute skin toxicity rates during or up to 3 months after radiotherapy are shown in Table 4. No significant differences in overall skin toxicity rates were observed

Fig. 3. Initial and residual interfraction and intrafraction translational displacements for all patients. Outliers, defined as observations greater than 1.5 times the interquartile range, are indicated with plus signs. ML = medial–lateral; CC = cranial–caudal; AP = anterior–posterior; SM = standard mask; SSM = skin-sparing mask.

Table 3. Pooled setup reproducibility for each mask group as SDs (and maximum error)

	Initial interfraction error		Residual interfraction error		Residual intrafraction error	
	SM	SSM	SM	SSM	SM	SSM
ML (mm)	1.7 (7.4)	1.4 (4.9)	1.4 (4.9)	1.3 (3.7)	0.8 (2.4)	0.9 (2.7)
CC (mm)	1.6 (5.0)	2.2 (9.5)	1.5 (4.5)	1.6 (5.1)	0.9 (3.3)	0.8 (3.8)
AP (mm)	1.7 (6.5)	1.8 (5.7)	1.5 (6.0)	1.5 (4.2)	1.0 (2.9)	1.1 (2.8)
Pitch (°)	1.2 (4.0)	1.1 (6.0)	1.2 (4.0)	1.0 (6.0)	0.7 (2.0)	0.6 (2.0)
Roll (°)	1.6 (5.9)	1.0 (3.5)	1.5 (5.5)	1.0 (3.5)	0.8 (1.9)	1.0 (3.0)
Yaw (°)	1.2 (3.5)	1.1 (4.0)	1.2 (3.5)	1.1 (4.0)	0.7 (2.5)	0.8 (3.6)

Abbreviations: SM = standard mask; SSM = skin-sparing mask; ML = medial–lateral; CC = cranial–caudal; AP = anterior–posterior.

(p = 0.35) between the SM and SSM groups. The highest grade of skin toxicity within the skin cutout regions, however, was lower compared with regions adjacent to the cutouts, underneath the mask. Examples of this effect are shown in clinical photos of patients treated with the SSM at the completion of therapy (Fig. 4).

DISCUSSION

Two immobilization masks for head-and-neck IMRT were prospectively evaluated in a randomized study of head-and-neck IMRT patients who underwent daily CBCT image guidance. Initial interfraction random errors (σ) ranged from 1.3 to 2.0 mm and systematic errors from 0.8 to 1.1 mm for both masks. Interfraction residual random error (σ) was 1.5 mm or less in each direction for both masks, and rotational error was less than 1°. Initial and residual interfraction systematic errors (Σ) were small for both masks, in general 1 mm or less and less than 1°. Intrafraction random and systematic errors were also small (<1 mm and <1°) for both masks, similar to measurement error. Reproducibility and stability were not significantly different for these masks. Thus low neck cutouts have been introduced as SMs for patients in our clinic receiving image-guided IMRT for head-and-neck cancer.

Boda-Heggemann *et al.* (15) evaluated head-and-neck immobilization masks using CBCT scans over a few fractions. They reported mean (SD) initial interfraction error in the neck region for a head-only thermoplastic mask as 2.1 mm (3.0 mm), 4.1 mm (5.2 mm), and 1.4 mm (3.9 mm) in the ML, CC, and AP directions, respectively. Similarly, rotations were −0.2° (2.3°), −1.3° (2.7°), and −1.1° (2.0°) for pitch, roll, and yaw, respectively. Our results compare favorably, perhaps due in part to the use of head-and-shoulder masks with chest tattoos and daily IGRT at our center.

Although statistically significant improvements in overall highest grade of skin toxicity were not seen with the use of the SSM, this is in part because of variability in the specific treatments (Table 1) and the fact that the entire mask was

Table 4. Highest-graded acute skin toxicity during and up to 3 months after radiotherapy

RTOG grade	SM [No. (%)]	SSM [No. (%)]
0	0	0
1	5 (45.5)	6 (66.7)
2	4 (36.4)	3 (33.3)
3	2 (18.2)	0

Abbreviation: RTOG = Radiation Therapy Oncology Group; SM = standard mask; SSM = skin-sparing mask.

Fig. 4. Skin toxicity for 2 patients in the skin-sparing mask (SSM) at the completion of intensity-modulated radiation therapy. Patients were prescribed 60 Gy in 30 fractions to primary disease with neck volumes receiving 54 Gy (top) and 64 Gy in 40 fractions twice daily with neck nodes receiving 46 Gy (bottom). Regions of less toxicity (arrows) are associated with areas under cutouts (corresponding masks are shown in Fig. 1).

not cut out. So, although the highest grade of toxicity may not differ, the surface area of skin toxicity may be reduced with the use of mask cutouts. This was not prospectively quantified because staff members were not instructed to assess toxicity specifically in cutout regions. Similar studies should provide better control for the variability in spatial toxicity assessments. Examples of reduced skin toxicity underlying the mask cutouts with SSMs are shown in Fig. 4. Skin toxicity has previously been evaluated in a randomized trial evaluating thermoplastic head masks vs. head-and-shoulder masks (11). The head-and-shoulder group had significantly more acute skin toxicity for patients receiving 60 Gy or greater.

Contouring the skin as a sensitive structure and assigning dose constraints at planning may reduce beam fluence directed toward the skin (22, 27, 28), which may reduce skin toxicity after IMRT, but optimal solutions for skin sparing without increasing the risk of recurrence are not clearly defined. The risk of intrafraction error may increase as treatment time lengthens for complex delivery such as IMRT (29), and thus skin-sparing solutions need to consider setup error.

Cone-beam CT was valuable in evaluating 3D setup error in 6 *df* in our patient population. Daily CBCT image guidance allowed large random setup errors to be detected and corrected online and systematic errors to be corrected offline. The optimal frequency and strategies for image guidance are not clearly established, but simple strategies such as correcting for setup error based on vertebral body position can reduce residual error (30–32). Measuring population setup data is important when new techniques are introduced into clinic, such as new immobilization devices, because the setup error will impact planning target volume margins (33).

Daily CBCT imaging can also be used to measure variability in position, shape, or volume, within the same patient over a treatment course, due to deformations of spine, weight loss, or disease response (16, 34). Zhang *et al.* (34) showed that head-and-neck bones can vary in position relative to one another up to 6 mm. We reported the displacements of the vertebral bodies about a single point (the isocenter typically in the mid neck) to easily compare mask differences. Interestingly, Zhang *et al.* also compared head masks with head-and-shoulder masks and found that C6 vertebra setup errors did not significantly differ. Soft-tissue variation was not the focus of this study, but we hypothesize that change in the soft tissues would not be different in SSMs or SMs, because we noticed no differences in the residual setup. Assessment of soft-tissue change and deformations observed during IGRT are the focus of other studies (35, 36).

A limitation of the intrafraction setup error measurements in this study is that a sample of pretreatment and post-treatment CBCT scans were evaluated as a surrogate for all change that may occur during the actual megavoltage beam delivery. Real-time monitoring was not available at the time of this study, although we speculate that the change between pre- and post-IMRT CBCT images represents a large component of intrafraction setup change. Devices that can monitor movements during beam delivery, such as optical tracking devices (10), would be complementary to the volumetric images provided by daily CBCT image guidance. Some authors have suggested that thermoplastic head-and-neck immobilization can perform as well as that used for stereotactic radiotherapy when combined with CBCT image guidance (15). Provided intrafraction motion is managed, interfraction reproducibility may become less important as online adaptive radiotherapy becomes available in the clinic for head-and-neck cancer patients (37, 38).

CONCLUSIONS

There were no significant changes in interfraction and intrafraction setup errors in head-and-neck cancer patients randomized to treatment with thermoplastic SSMs vs. SMs, as evaluated with daily CBCT. On the basis of the results of this study, cutout masks are being recommended for all of our head-and-neck cancer patients treated with IMRT and daily CBCT IGRT.

REFERENCES

1. Lin A, Kim HM, Terrell JE, *et al*. Quality of life after parotid-sparing IMRT for head-and-neck cancer: A prospective longitudinal study. *Int J Radiat Oncol Biol Phys* 2003;57:61–70.
2. Pow EH, Kwong DL, McMillan AS, *et al*. Xerostomia and quality of life after intensity-modulated radiotherapy vs. conventional radiotherapy for early-stage nasopharyngeal carcinoma: Initial report on a randomized controlled clinical trial. *Int J Radiat Oncol Biol Phys* 2006;66:981–991.
3. Hong TS, Tome WA, Chappell RJ, *et al*. The impact of daily setup variations on head-and-neck intensity-modulated radiation therapy. *Int J Radiat Oncol Biol Phys* 2005;61: 779–788.
4. Siebers JV, Keall PJ, Wu Q, *et al*. Effect of patient setup errors on simultaneously integrated boost head and neck IMRT treatment plans. *Int J Radiat Oncol Biol Phys* 2005;63: 422–433.
5. Bentel GC, Marks LB, Hendren K, *et al*. Comparison of two head and neck immobilization systems. *Int J Radiat Oncol Biol Phys* 1997;38:867–873.
6. Engelsman M, Rosenthal SJ, Michaud SL, *et al*. Intra- and interfractional patient motion for a variety of immobilization devices. *Med Phys* 2005;32:3468–3474.
7. Gilbeau L, Octave-Prignot M, Loncol T, *et al*. Comparison of setup accuracy of three different thermoplastic masks for the treatment of brain and head and neck tumors. *Radiother Oncol* 2001;58:155–162.
8. Humphreys M, Guerrero Urbano MT, Mubata C, *et al*. Assessment of a customised immobilisation system for head and neck IMRT using electronic portal imaging. *Radiother Oncol* 2005; 77:39–44.
9. Hurkmans CW, Remeijer P, Lebesque JV, *et al*. Set-up verification using portal imaging; review of current clinical practice. *Radiother Oncol* 2001;58:105–120.
10. Kim S, Akpati HC, Kielbasa JE, *et al*. Evaluation of intrafraction patient movement for CNS and head & neck IMRT. *Med Phys* 2004;31:500–506.
11. Sharp L, Lewin F, Johansson H, *et al*. Randomized trial on two types of thermoplastic masks for patient immobilization during

radiation therapy for head-and-neck cancer. *Int J Radiat Oncol Biol Phys* 2005;61:250–256.
12. Willner J, Hadinger U, Neumann M, *et al*. Three dimensional variability in patient positioning using bite block immobilization in 3D-conformal radiation treatment for ENT-tumors. *Radiother Oncol* 1997;43:315–321.
13. Li H, Zhu XR, Zhang L, *et al*. Comparison of 2D radiographic images and 3D cone beam computed tomography for positioning head-and-neck radiotherapy patients. *Int J Radiat Oncol Biol Phys* 2008;71:916–925.
14. Fuss M, Salter BJ, Cheek D, *et al*. Repositioning accuracy of a commercially available thermoplastic mask system. *Radiother Oncol* 2004;71:339–345.
15. Boda-Heggemann J, Walter C, Rahn A, *et al*. Repositioning accuracy of two different mask systems—3D revisited: Comparison using true 3D/3D matching with cone-beam CT. *Int J Radiat Oncol Biol Phys* 2006;66:1568–1575.
16. Barker JL Jr., Garden AS, Ang KK, *et al*. Quantification of volumetric and geometric changes occurring during fractionated radiotherapy for head-and-neck cancer using an integrated CT/linear accelerator system. *Int J Radiat Oncol Biol Phys* 2004;59:960–970.
17. Hadley SW, Kelly R, Lam K. Effects of immobilization mask material on surface dose. *J Appl Clin Med Phys* 2005;6:1–7.
18. Fiorino C, Cattaneo GM, del Vecchio A, *et al*. Skin dose measurements for head and neck radiotherapy. *Med Phys* 1992;19:1263–1266.
19. Fiorino C, Cattaneo GM, Del Vecchio A, *et al*. Skin-sparing reduction effects of thermoplastics used for patient immobilization in head and neck radiotherapy. *Radiother Oncol* 1994;30:267–270.
20. Mellenberg DE. Dose behind various immobilization and beam-modifying devices. *Int J Radiat Oncol Biol Phys* 1995;32:1193–1197.
21. Halm EA, Tamri A, Bridier A, *et al*. Influence of thermoplastic masks on the absorbed skin dose for head and neck tumor radiotherapy [In French]. *Cancer Radiother* 2002;6:310–319.
22. Lee N, Chuang C, Quivey JM, *et al*. Skin toxicity due to intensity-modulated radiotherapy for head-and-neck carcinoma. *Int J Radiat Oncol Biol Phys* 2002;53:630–637.
23. Carl J, Vestergaard A. Skin damage probabilities using fixation materials in high-energy photon beams. *Radiother Oncol* 2000;55:191–198.
24. Weltens C, Kesteloot K, Vandevelde G, *et al*. Comparison of plastic and Orfit masks for patient head fixation during radiotherapy: Precision and costs. *Int J Radiat Oncol Biol Phys* 1995;33:499–507.
25. Jaffray DA, Siewerdsen JH. Cone-beam computed tomography with a flat-panel imager: Initial performance characterization. *Med Phys* 2000;27:1311–1323.
26. van Herk M. Errors and margins in radiotherapy. *Semin Radiat Oncol* 2004;14:52–64.
27. Thomas SJ, Hoole AC. The effect of optimization on surface dose in intensity modulated radiotherapy (IMRT). *Phys Med Biol* 2004;49:4919–4928.
28. Court LE, Tishler RB. Experimental evaluation of the impact of different head-and-neck intensity-modulated radiation therapy planning techniques on doses to the skin and shallow targets. *Int J Radiat Oncol Biol Phys* 2007;69:607–613.
29. Linthout N, Verellen D, Tournel K, *et al*. Six dimensional analysis with daily stereoscopic x-ray imaging of intrafraction patient motion in head and neck treatments using five points fixation masks. *Med Phys* 2006;33:504–513.
30. de Boer HC, van Sornsen de Koste JR, Senan S, *et al*. Analysis and reduction of 3D systematic and random setup errors during the simulation and treatment of lung cancer patients with CT-based external beam radiotherapy dose planning. *Int J Radiat Oncol Biol Phys* 2001;49:857–868.
31. Zeidan OA, Langen KM, Meeks SL, *et al*. Evaluation of image-guidance protocols in the treatment of head and neck cancers. *Int J Radiat Oncol Biol Phys* 2007;67:670–677.
32. de Boer HC, Heijmen BJ. A protocol for the reduction of systematic patient setup errors with minimal portal imaging workload. *Int J Radiat Oncol Biol Phys* 2001;50:1350–1365.
33. Prisciandaro JI, Frechette CM, Herman MG, *et al*. A methodology to determine margins by EPID measurements of patient setup variation and motion as applied to immobilization devices. *Med Phys* 2004;31:2978–2988.
34. Zhang L, Garden AS, Lo J, *et al*. Multiple regions-of-interest analysis of setup uncertainties for head-and-neck cancer radiotherapy. *Int J Radiat Oncol Biol Phys* 2006;64:1559–1569.
35. Brock KK, Hawkins M, Eccles C, *et al*. Improving image-guided target localization through deformable registration. *Acta Oncol* 2008;47:1279–1285.
36. Tward DJ, Siewerdsen JH, Daly MJ, *et al*. Soft-tissue detectability in cone-beam CT: Evaluation by 2AFC tests in relation to physical performance metrics. *Med Phys* 2007;34:4459–4471.
37. Sharpe MB, Brock KK, Rehbinder H, *et al*. Adaptive planning and delivery to account for anatomical changes induced by radiation therapy of head and neck cancer [Abstract]. *Int J Radiat Oncol Biol Phys* 2005;63(Suppl. 1):S3.
38. Court LE, Tishler RB, Petit J, *et al*. Automatic online adaptive radiation therapy techniques for targets with significant shape change: A feasibility study. *Phys Med Biol* 2006;51:2493–2501.